Chemical Science

Accepted Manuscript

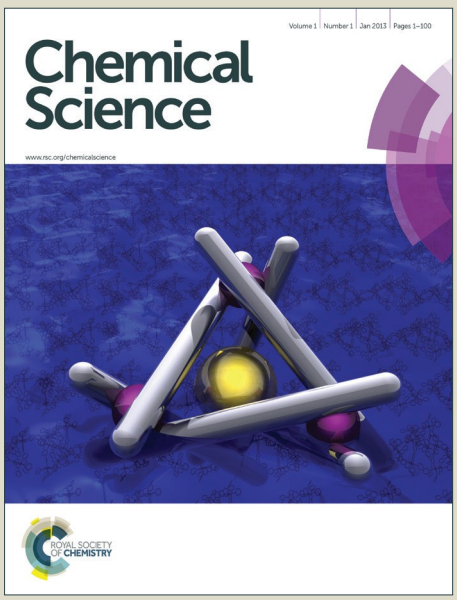

ROYAL SOCIETY OF CHEMISTRY

www.rsc.org/chemicalscience

Chemical Science

View Article Online
DOI: 10.1039/C6SC00055J

ARTICLE

FRET Probe with AIEgen as the Energy Quencher: Dual Signal Turn-On for Self-Validated Caspase Detection

Received 00th January 20xx,
Accepted 00th January 20xx

DOI: 10.1039/x0xx00000x

www.rsc.org/

Youyong Yuan,[a,†] Ruoyu Zhang,[a,†] Xiamin Cheng,[a,†] Shidang Xu,[a] and Bin Liu[a,b,*]

Accurate detection of biological substance is highly desirable to study various biological processes and evaluate disease progression. Herein, we report a self-validated fluorescent probe which is composed of a coumarin fluorophore as energy donor and a fluorogen with aggregation-induced emission characteristics (AIEgen) as energy quencher linked through a caspase-3 specific peptide substrate. Unlike the traditionally widely studied fluorescence resonance energy transfer (FRET) probes, our new generation of FRET probe itself is non-fluorescent due to energy transfer as well as the dissipation of the acceptor energy through free molecular motion of the AIEgen. Upon interaction with caspase-3, the probe displays strong green and red fluorescent signals synchronously due to the separation of donor-quencher and aggregation of the released AIEgen. The fluorescence turn-on with dual signal amplification allows real-time and self-validated enzyme detection with high signal-to-background ratio, providing a good opportunity to accurately monitor various biological processes in real-time manner.

Introduction

Fluorescent probes have attracted increasing attention in biomedical research due to their high sensitivity, good selectivity, non-invasiveness and the capability of real-time detection.[1] Fluorescence turn-on probes are superior to turn-off probes due to their lower background signal and higher signal output.[2] Fluorescence resonance energy transfer (FRET) is one of the most widely exploited mechanisms for the design of fluorescence turn-on probes, which have been successfully utilized in sensing, imaging, environmental monitoring, and medical diagnosis.[3] Two strategies have been generally utilized to design FRET probes. One is to conjugate a fluorescent dye with a quencher (donor-quencher model) and the other is to link two fluorescent dyes which can form the donor-acceptor pair (donor-acceptor model).[4] Once these FRET probes are exposed to analytes, the separation between the donor and quencher/acceptor leads to readable signals. While the donor-quencher model exhibits single fluorescent signal output, the donor-acceptor model shows donor fluorescence turn-on at the expense of the acceptor emission. The single fluorescent signal turn-on can only provide limited information, which is sometimes insufficient for accurate detection.[5] Recently, several "always on" probes with different image modalities have been developed for self-validated bioimaging in order to provide more accurate results.[5] Up to now, a variety of biological probes based on fluorescence imaging, magnetic resonance imaging (MRI), positron emission tomography (PET) and photoacoustic imaging have been actively explored to offer dual signal output in one study.[6] However, single fluorescence turn-on probe with dual signal output upon encountering specific analyte have not been reported yet. It is thus of great interest to develop single fluorescent probes with dual signal turn-on at different emission wavelengths for self-validated sensing and imaging, which remains challenging.

In Recent years, fluorogens with aggregation-induced emission characteristics (AIEgens) have attracted considerable attention in biosensing and bioimaging.[7] Opposite to traditional fluorophores that show a notorious phenomenon known as aggregation-caused quenching (ACQ),[8] AIEgens are non-emissive in molecularly dissolved state but can be induced to emit strongly in aggregates due to the restriction of intramolecular motion (RIM) and prohibition of energy dissipation *via* non-radiative channels.[9] Based on this unique property, several fluorescence turn-on probes have been developed for detection and imaging of various analytes.[7c] These probes are generally based on AIEgens conjugated to hydrophilic recognition elements. When the AIE probes are well-dissolved in aqueous media, the background fluorescence is very low. Upon specific analyte recognition, the probes are cleaved to release the hydrophobic AIEgens and yield bright fluorescence. As compared to traditional FRET probes which require dual labelling to realize fluorescence turn-on, these singly labelled AIE probes show high simplicity, which makes them very useful in the development of multifunctional probes

[a] Department of Chemical and Biomolecular Engineering, National University of Singapore, 4 Engineering Drive 4, Singapore 117585, E-mail: cheliub@nus.edu.sg
[b] Institute of Materials Research and Engineering, Agency for Science, Technology and Research (A*STAR), 3 Research Link, Singapore, 117602
† These authors contributed equally to this work.
Electronic Supplementary Information (ESI) available: [details of any supplementary information available should be included here]. See DOI: 10.1039/x0xx00000x

View Article Online
DOI: 10.1039/C6SC00055J

for monitoring of multiple processes in one go.[7c] These successful examples have motivated us to explore whether the energy dissipation of AIEgens could affect other fluorophores conjugated to the probe. In this case, it would offer a new generation of energy quenchers, which is able to fluoresce once it is separated from the energy donor and offers for the first time a dual signal turn-on probe for self-validated biosensing and bioimaging.

As a proof of concept, in this contribution, we report a fluorescent probe based on coumarin (Cou) as energy donor and an AIEgen as the energy quencher conjugated via a Asp-Glu-Val-Asp (DEVD) substrate for caspase-3 detection (Scheme 1).[10] The probe itself is non-fluorescent due to the energy transfer and dissipation of the acceptor energy through free motion of AIEgens. Upon addition of caspase-3, it displays strong green fluorescence of Cou due to the separation of donor-acceptor and intense red fluorescence of AIEgen due to the aggregation of the released AIEgen residue. This dual fluorescent signal turn-on can be used for caspase-3 detection both in solution and in cells, which opens new avenues for the development of next generation self-validated FRET probes with high signal-to-background ratio and fluorescence amplification.

Results and discussion

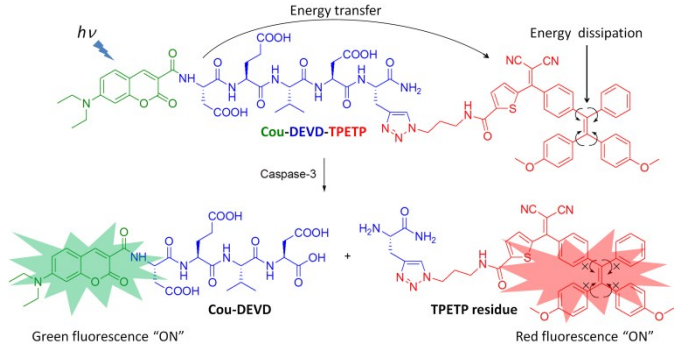

Scheme 1. Schematic illustration of the FRET probe using AIEgen as energy quencher with dual signal output for self-validated caspase-3 detection.

Recently, some AIEgens with red emission has been developed for bioimaging and tetraphenylethenethiophene (TPETP) was selected for this study.[11] The synthetic route to the azide-functionalized TPETP (TPETP-N_3) and the probe Cou-DEVD-TPETP are shown in Scheme 2. Compound **1** was synthesized by McMurry reaction between bis(4-methoxyphenyl)methanone and (4-bromophenyl)(phenyl)methanone in the presence of $TiCl_4$ and Zn. Subsequently, compound **1** was reacted with compound **2** in the presence of butyllithium to yield compound **3**. The carboxyl group of compound **3** was deprotected by sodium hydroxide in methanol-water mixture, which was further reacted with 3-azidopropan-1-amine to yield compound **5**. Compound **5** was further reacted with malononitrile on SiO_2

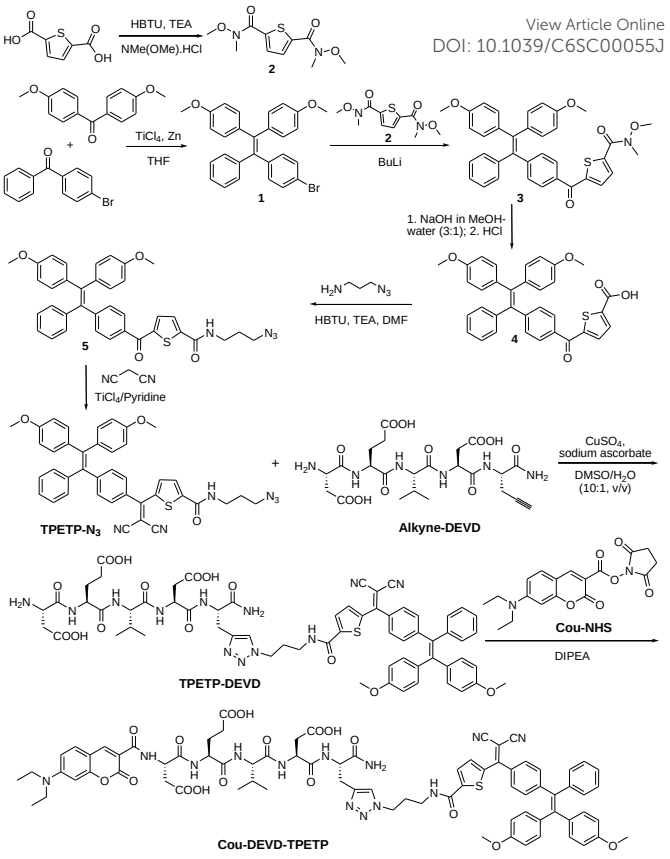

Scheme 2. Synthetic route to the probe of Cou-DEVD-TPETP. HBTU: *O*-(benzotriazol-1-yl)-*N,N,N′,N′*-tetramethyluronium hexafluorophosphate; TEA: triethylamine; $TiCl_4$: titanium(IV) chloride; Zn: zinc; THF: tetrahydrofuran; BuLi: butyllithium; DMF: *N*, *N*-dimethylformamide; DIPEA: *N*, *N*-diisopropylethylamine; Cou-NHS: 7-(diethylamino)coumarin-3-carboxylic acid *N*-succinimidyl ester.

support to produce azide-functionalized TPETP (TPETP-N_3). The "click" reaction between TPETP-N_3 and alkyne-functionalized DEVD catalyzed by copper(II) sulfate ($CuSO_4$) and sodium ascorbate (NaAsc) afforded amine terminated TPETP-DEVD which was further reacted with 7-(diethylamino)coumarin-3-carboxylic acid *N*-succinimidyl ester (Cou-NHS) in the presence of *N*, *N*-diisopropylethylamine (DIPEA) to afford Cou-DEVD-TPETP in 52% yield after HPLC purification. Detailed characterization data are shown in Figures S1-S8. The AIE property of TPETP-N_3 was confirmed by studying its PL spectra in DMSO or DMSO/water mixtures (v/v = 1/99). As shown in Figure S9A, TPETP-N_3 is almost non-fluorescent in DMSO which should be due to the easy intramolecular motions of the TPE phenyl rings in benign solvents.[7a] However, TPETP-N_3 in DMSO/water mixtures (v/v = 1/99) is highly fluorescent, which shows 110-fold brighter fluorescence than that in DMSO. The increase in fluorescence intensity is attributed to the aggregation of TPETP-N_3, which restricts the intramolecular motion when the water fraction is increased. The formation of TPETP-N_3 aggregates in aqueous media was also confirmed by laser light scattering (LLS) measurements and transmission electron microscopy (TEM) image (Figure S9), while there is no

View Article Online
DOI: 10.1039/C6SC00055J

LLS signal detected in DMSO solution. The absorption and emission spectra of Cou and TPETP-N_3 are shown in Figure S10. The emission of Cou and the absorption of TPETP-N_3 shows a perfect spectral overlap, indicating that they could form an energy transfer pair.

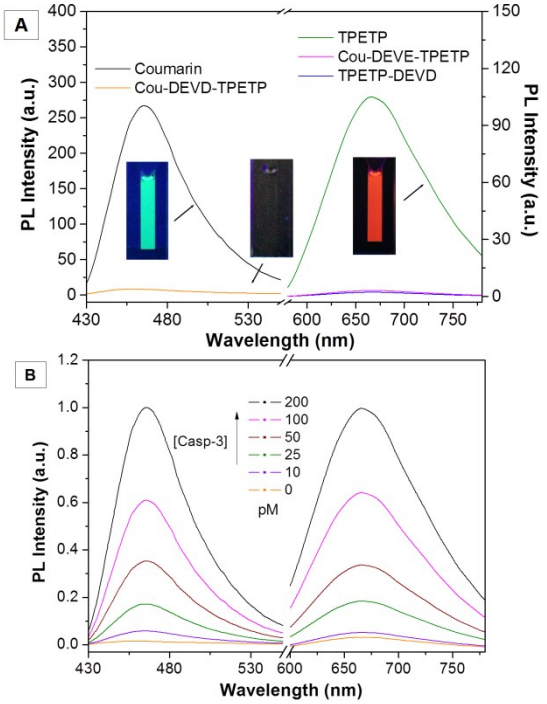

Figure 1. (A) Photoluminescence (PL) spectra of Cou, TPETP-N_3 and Cou-DEVD-TPETP (10 μM) in DMSO/PBS buffer (v/v = 1/99). (B) PL spectra of Cou-DEVD-TPETP (10 μM) upon incubation with different concentrations of caspase-3 (λ_{ex}: 405 nm, emission collected from 430 – 550 nm is from the Cou-DEVD and that at 600 – 780 nm is from the TPETP residue).

To validate the energy transfer between Cou and TPETP-N_3, the optical properties of Cou, TPETP-N_3 and Cou-DEVD-TPETP were studied in DMSO/PBS buffer (v/v = 1/99). Cou and TPETP-N_3 have absorption maxima at 445 and 470 nm, with emission maxima at 465 and 665 nm, respectively (Figure S10). As both Cou and TPETP-N_3 show obvious absorption at 405 nm, it offers the possibility of dual signal collection upon a single wavelength excitation. As shown in Figure 1A, upon excitation at 405 nm, both Cou and TPETP-N_3 are highly fluorescent while Cou-DEVD-TPETP emits very weakly, which indicates that the probe has extremely low background signal as designed. The rationale behind the fluorescence quenching of Cou and TPETP parts in the probe is due to energy transfer from the former to the latter, and the dissipation of the AIEgen energy through free motion of the molecules. The fluorescence of the probe remains weak in aqueous media with different ionic strength or in cell culture medium (Figure S11). Upon addition of caspase-3, the cleavage of DEVD separates Cou-DEVD away from the proximity of TPETP. This leads to the recovery of the green fluorescence of Cou and synchronously allows the formation of TPETP residue aggregates with red fluorescence turn-on. As shown in Figure 1B, upon treatment with caspase-3 at different concentrations for 1 h at 37 °C, the emissions of Cou-DEVD and TPETP residue exhibit concentration-dependent turn-on at 465 nm and 665 nm, respectively. When the probe was treated with 200 pM caspase-3 for 1 h, the fluorescence of Cou-DEVD and TPETP residue showed 55 and 37 fold increase compared to their intrinsic emission in the probe, respectively. In addition, the peak PL intensities of Cou and TPETP are shown in Figure S12, which correlate linearly to the concentration of caspase-3 with R^2 = 0.97, indicating that the enzyme concentration can be quantified and self-validated through monitoring the PL intensity changes of Cou and TPETP. In addition, in the presence of caspase-3 inhibitor 5-[(S)-(+)-2-(methoxymethyl)pyrrolidino] sulfonylisatin, the probe remains weakly emissive even after the treatment with caspase-3. The kinetic analysis of the enzymatic reaction was also studied by incubating casp-3 with different concentrations of Cou-DEVD-TPETP at 37 °C. As shown in Figure S13, the Michaelis constants (K_M) and the kinetic constants (k_{cat}) were calculated to be 7.70 μM and 2.69 s^{-1}, which are comparable to the previous FRET probe.[10a] The specific cleavage of DEVD by caspase-3 was further confirmed by reverse phase HPLC and mass spectrometry study through the formation of Cou-DEVD and TPETP residue (Figure S14).

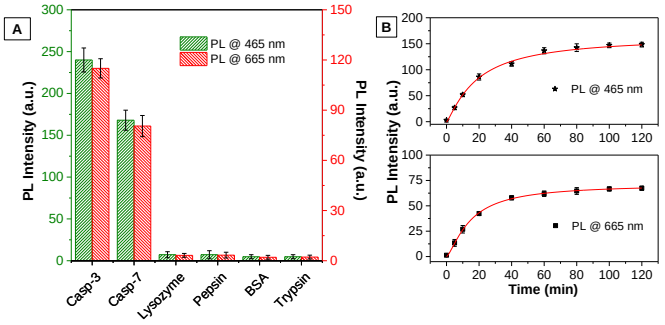

Figure 2. (A) PL intensities monitored at both 465 and 665 nm for Cou-DEVD-TPETP (10 μM) upon treatment with various proteins; (B) Time-dependent PL intensities for Cou-DEVD-TPETP (10 μM) upon addition of caspase-3 (λ_{ex}: 405 nm).

The selectivity of the probe was studied by incubating the probe with different caspase enzymes as well as several proteins including lysozyme, pepsin, bovine serum albumin and trypsin. As shown in Figure 2A and Figure S15A, only the probe treated with caspase-3/-7 displays significant fluorescence increase, confirming the specificity of the probe for caspase-3/-7. The time-dependent fluorescence change of the probe after incubation with caspase-3/-7 and cell lysate of normal and apoptotic cells were also studied. As shown in Figure 2B, a quick and steady fluorescence increase at both 465 and 665 nm is observed when caspase-3 is added. On the other hand, the HeLa cells were induced to undergo apoptosis by the treatment of staurosporine (STS), a commonly used apoptosis inducer,[12] and the cell lysates were incubated with the probe. As shown in Figure S15, the fluorescent signals at both wavelengths increase along with incubation time which are similar to the solution study shown in Figure 2B. In contrast, no fluorescence change is observed when the probe

View Article Online
DOI: 10.1039/C6SC00055J

is incubated with HeLa cell lysate without STS treatment, indicating that the probe is stable with cellular proteins and it can be specifically recognized by caspase enzyme with self-validation.

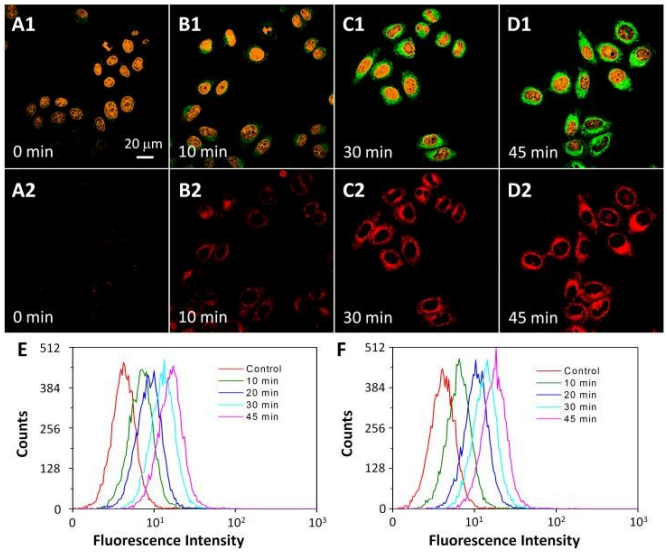

Figure 3. Confocal images of Cou-DEVD-TPETP (10 μM) incubated HeLa cells upon treatment with STS (1 μM) for different time. Green fluorescence (Cou-DEVD, E_x: 405 nm; E_m: 505-525 nm); orange fluorescence (nucleus dyed with SYTO® orange, E_x: 543 nm, E_m: 610-640 nm); A1-D1 are the overlay images of the fluorescence of Cou and SYTO® orange; red fluorescence (TPETP residue, A2-D2, E_x: 405 nm, E_m: > 650 nm). (E, F) Flow cytometric analysis of Cou-DEVD (E) and TPETP residue (F) fluorescence in HeLa cells after treatment with STS (1 μM).

To explore the potential of using Cou-DEVD-TPETP for caspase imaging in live cells, the probe was incubated with HeLa and MDA-MB-231 cells and subsequently treated with STS. The fluorescence changes at both wavelgnths were monitored by confocal laser scanning microscopy. As shown in Figure 3 and Figure S16, the fluorescent signals of Cou-DEVD and TPETP residue increase gradually and synchronously with the cellular apoptotic progress upon addition of STS. The fluorescence changes after STS treatment were also confirmed by flow cytometric analysis (Figures 3E and 3F). These results clearly support that the probe with dual signal turn-on can be used for self-validation of caspase-3 activation and for real-time monitoring of apoptosis process in live cells.

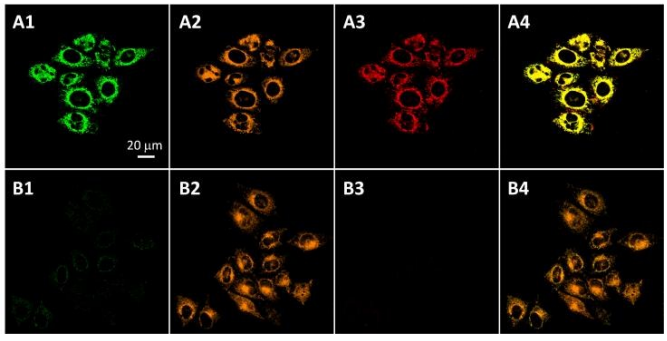

Figure 4. Confocal images of apoptotic HeLa cells treated with Cou-DEVD-TPETP (10 μM) in the absence (A) and (B) presence of caspase-3 inhibitor and stained with anti-caspase-3 primary antibody and a Texas Red-labeled secondary antibody. Green fluorescence (Cou-DEVD, A1, B1, E_x: 405 nm; E_m: 505-525 nm); orange fluorescence (Texas Red, A2, B2, E_x: 543 nm, E_m: 610–640 nm); red fluorescence (TPETP residue, A3, B3, E_x: 405 nm, E_m: > 650 nm); A4, B4 are the overlay images of A1-A3 and B1-B3, respectively. Due to the low absorbance of TPETP at 543 nm, its emission spectral overlap with Texas Red is negligible.

To further confirm that the probe can image cell apoptosis, HeLa cells were co-stained with anti-caspase-3 primary antibody and a Texas Red-labeled secondary antibody. As shown in Figure 4A, the fluorescence of Cou-DEVD and TPETP residue in HeLa cells with STS treatment overlaps well with the immunofluorescence signals from Texas Red. However, when the cells are pretreated with caspase-3/-7 inhibitor, both intensities are greatly reduced while the fluorescence of Texas Red remains (Figure 4B). This is because the activity of caspase-3/-7 enzyme is prohibited upon inhibitor treatment, but the apoptosis process is not affected. Similar results were also observed in MDA-MB-231 cells (Figure S17). Overall, these results further confirm the caspase-3/-7 specific turn-on of the probe fluorescence in cells.

It is known that most drugs induce cell death through apoptosis pathway.[13] To verify the potential of this probe for self-validated drug screening, the probe incubated cells were treated with several cell apoptosis inducing drugs and the apoptosis-inducing capabilities were evaluated by monitoring the fluorescent signal changes. As shown in Figure 5, the strongest fluorescence of Cou-DEVD and TPETP residue is observed when the cells are treated with STS, while moderate fluorescence is observed when the cells are treated with the anticancer drug of doxorubicin (DOX) or cisplatin. The cells treated with Na Asc show the lowest fluorescence, indicating Na Asc is not a good apoptosis inducer. Similar results were also observed in MDA-MB-231 cells (Figure S18), revealing the generality of the probe. To test whether the probe could be used to quantify the capability of different drugs in inducing cell apoptosis, the cells were further treated with different amount of Na Asc, cisplatin, DOX and STS and the fluorescent signals were studied. As shown in Figure 5C, the fluorescent signals of Cou-DEVD and TPETP residue intensify synchronously with the drug concentration for all the four drugs. It should be noted that the probe (up to 25 μM) do not show any obvious cytotoxicity to both cells after 48 h incubation (Figure S19). Collectively, these results indicate that Cou-DEVD-TPETP can quantitatively analyze the capability of different drugs to induce cell apoptosis in living cells with self-validation, which offers a new opportunity to accurately evaluate the efficiency of new anticancer drugs.

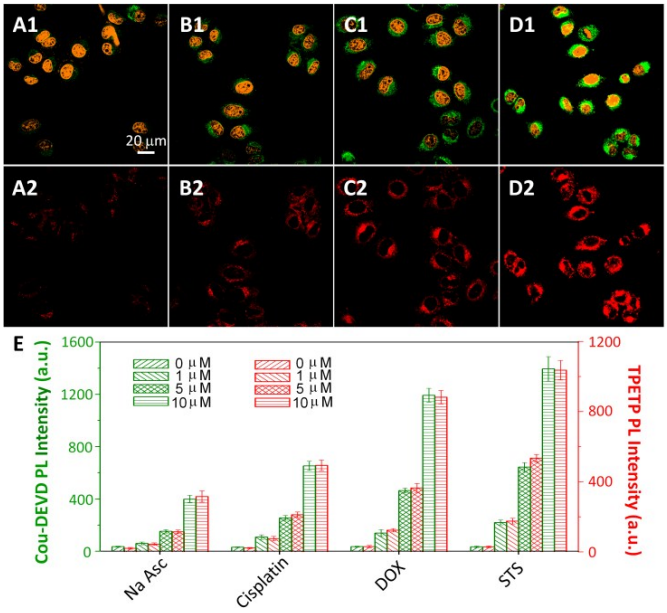

Figure 5. Confocal images of Cou-DEVD-TPETP (10 μM) incubated HeLa cells upon treatment with (A) sodium ascorbate (Na Asc), (B) cisplatin, (C) DOX and (D) STS. Green fluorescence (Cou-DEVD, E_x: 405 nm; E_m: 505-525 nm); orange fluorescence (nucleus dyed with SYTO® orange, E_x: 543 nm, E_m: 610-640 nm); A1-D1 are the overlay images of the fluorescence of Cou and SYTO® orange; red fluorescence (TPETP residue, A2-D2, E_x: 405 nm, E_m: > 650 nm). (E) PL intensities of Cou-DEVD and TPETP residue in HeLa cells treated with of Na Asc, cisplatin, DOX and STS at different concentrations.

Conclusions

In summary, we developed a simple but unique fluorescent probe with dual signal turn-on for accurate caspase-3 detection with self-validation. Thanks to the unique property of the AIEgen, the fluorescence of the probe is initially quenched, but two-signal turn-on is produced upon interaction with caspase-3 enzyme. The dual-signal turn-on enables real-time monitoring of caspase-3 activity in solution and in live cells with high efficiency, which has been utilized for self-validated enzyme detection and drug screening. Compared to traditional FRET probes that show single fluorescence turn-on upon interaction with the analytes, the probe developed in this work using AIEgen as the energy quencher does not complicate the probe design, but offers for the first time two-signal turn-on upon analyte recognition. In addition, this is the first time that the energy quencher could change its role to a signal reporter upon analyte recognition. Our design strategy of AIEgen based FRET probe can be generalized to other probes simply by changing DEVD to other cleavable substrate, which will open new avenues for self-validated diagnosis, imaging and drug screening applications. Potential translation would still be needed to evaluate the *in vivo* cytotocity and design probes with longer absorption wavelength.

Acknowledgements

We thank the Ministry of Defence (R279-000-340-232), SMART (R279-000-378-592), the Ministry of Education (R279-000-391-112), Singapore NRF Investigatorship (R279-000-444-281) and the Institute of Materials Research and Engineering of Singapore (IMRE/14-8P1110) for financial support.

References

1 (a) M. I. J. Stich, L. H. Fischer, O. S. Wolfbeis, *Chem. Soc. Rev.* 2010, **39**, 3102-3114; (b) Z. G. Yang, J. F. Cao, Y. X. He, J. H. Yang, T. Kim, X. J. Peng, J. S. Kim, *Chem. Soc. Rev.* 2014, **43**, 4563-4601; (c) J. Zheng, R. H. Yang, M. L. Shi, C. C. Wu, X. H. Fang, Y. H. Li, J. H. Li, W. H. Tan, *Chem. Soc. Rev.* 2015, **44**, 3036-3055.

2 J. Chan, S. C. Dodani, C. J. Chang, *Nat. Chem.* 2012, **4**, 973-984.

3 J. J. Li, F. F. Cheng, H. P. Huang, L. L. Li, J. J. Zhu, *Chem. Soc. Rev.* 2015, **44**, 7855-7880.

4 K. E. Sapsford, L. Berti, I. L. Medintz, *Angew. Chem. Int. Ed.* 2006, **45**, 4562-4588.

5 D. E. Lee, H. Koo, I. C. Sun, J. H. Ryu, K. Kim, I. C. Kwon, *Chem. Soc. Rev.* 2012, **41**, 2656-2672.

6 (a) B. E. Rolfe, I. Blakey, O. Squires, H. Peng, N. R. B. Boase, C. Alexander, P. G. Parsons, G. M. Boyle, A. K. Whittaker, K. J. Thurecht, *J. Am. Chem. Soc.* 2014, **136**, 2413–2419; (b) V. S. R. Harrison, C. E. Carney, K. W. MacRenaris, E. A. Waters, T. J. Meade, *J. Am. Chem. Soc.*, 2015, **137**, 9108–9116; (c) Y. Sun, X. W. Ma, K. Cheng, B. Y. Wu, J. L. Duan, H. Chen, L. H. Bu, R. P. Zhang, X. M. Hu, Z. X. Deng, L. Xing, X. C. Hong, Z. Cheng, *Angew. Chem. Int. Ed.* 2015, **54**, 5981–5984 (d) Y. H. Wang, S. Y. Song, J, H. Liu, D. P. Liu, H. J. Zhang, *Angew. Chem. Int. Ed.* 2015, **54**, 536–540; (e) X. J. Wu, B. J. Lin, M. Z. Yu, L. Yang, J. H. Han, S. F. Han, *Chem. Sci.* 2015, **6**, 2002-2009; (f) Q. Wu, Q. Cheng, S. Yuan, J. C. Qian, K. Zhong, Y. F. Qian, Y. Z. Liu, *Chem. Sci.* 2015, **6**, 6607-6613.

7 (a) J. Mei, N. L. C. Leung, R. T. K. Kwok, J. W. Y. Lam, B. Z. Tang, *Chem. Rev.* 2015, **115**, 11718-11940; (b) W. J. Guan, W. J. Zhou, C. Lu, B. Z. Tang *Angew. Chem. Int. Ed.* 2015, **54**, 15160-15164; (c) J. Liang, B. Tang, B. Liu, *Chem. Soc. Rev.* 2015, **44**, 2798-2811; (d) K. Li, B. Liu, *Chem. Soc. Rev.* 2014, **43**, 6570-6597; (e) X. Zhang, X. Zhang, L. Tao, Z. Chi, J. Xu, Y. Wei, *J. Mater. Chem. B* 2014, **2**, 4398-4414; (f) Q. L. Hu, M. Gao, G. X. Feng, B. Liu, *Angew. Chem. Int. Ed.* 2014, **53**, 14225-14229; (g) Y. Yuan, R. T. Kwok, B. Z. Tang, B. Liu, *J. Am. Chem. Soc.* 2014, **136**, 2546-2554; (h) S. Xu, Y. Yuan, X. Cai, C. Zhang, F. Hu, J. Liang, G. Zhang, D. Zhang, B. Liu. *Chem. Sci.* 2015, **6**, 5824-5830; (i) X. D. Xue, Y. Y. Zhao, L. R. Dai, X. Zhang, X. H. Hao, C. Q. Zhang, S. D. Huo, J. Liu, C. Liu, A. Kumar, W. Q. Chen, G. Z. Zou, X. J. Liang, *Adv. Mater.* 2014, **26**, 712-717; (j) Y. Y. Yuan, C. J. Zhang, M. Gao, R. Y. Zhang, B. Z. Tang, B. Liu, *Angew. Chem. Int. Ed.* 2015, **54**, 1780-1786; (k) A. D. Shao, Y. S. Xie, S. J. Zhu, Z. Q. Guo, S. Q. Zhu, J. Guo, P. Shi, T. D. James, H. Tian, W. H. Zhu, *Angew. Chem. Int. Ed.* 2015, **54**, 7275-7280; (l) Z. Xie, C. Chen, S. Xu, J. Li, Y. Zhang, S. Liu, J. Xu, Z. Chi, *Angew. Chem. Int. Ed.* 2015, **54**, 7181-7184.

8 J. B. Birks, Photophysics of Aromatic Molecules; Wiley: London, 1970.

9 Y. N. Hong, J. W. Y. Lam, B. Z. Tang, *Chem. Soc. Rev.* 2011, **40**, 5361-5388.

10 (a) K. Boeneman, B. C. Mei, A. M. Dennis, G. Bao, J. R. Deschamps, H. Mattoussi, I. L. Medintz, *J. Am. Chem. Soc.* 2009, **131**, 3828-3829; (b) J. F. Lovell, M. W. Chan, Q. C. Qi, J. Chen, G. Zheng, *J. Am. Chem. Soc.* 2011, **133**, 18580–18582; (c) L. Zhang, J. P. Lei, J. T. Liu, F. J. Ma, H. X. Ju, *Chem. Sci.*

View Article Online
DOI: 10.1039/C6SC00055J

2015, **6**, 3365-3372; (d) D. Ye, A. J. Shuhendler, P. Pandit, K. D. Brewer, S. S. Tee, L. Cui, G. Tikhomirov, B. Rutt, J. H. Rao, *Chem. Sci.* 2014, **5**, 3845–3852; (e) Z. Gu, A. Biswas, K. Joo, B. L. Hu, P. Wang, Y. Tang, *Chem. Commun.* 2010, **46**, 6467-6469.

11 (a) Y. Y. Huang, F. Hu, R. Zhao, G. X. Zhang, H. Yang, D. Q. Zhang, *Chem. Eur. J.* 2014, **20**, 158-164; (b) F. Hu, Y. Y. Huang, G. X. Zhang, R. Zhao, H. Yang, D. Q. Zhang, *Anal. Chem.* 2014, **86**, 7987–7995; (c) Y. Y. Yuan, C. Zhang, R. Kwok, S. Xu, R. Zhang, J. Wu, B. Z. Tang, B. Liu, *Adv. Funct. Mater.* 2015, **25**, 6586-6595; (d) Y. Y. Yuan, C. J. Zhang, B. Liu, *Angew. Chem. Int. Ed.* 2015, **54**, 11419-11423.

12 X. D. Zhang, S. K. Gillespie, P. Hersey, *Mol. Cancer Ther.* 2004, **3**, 187-197.

13 H. Okada, T. W. Mak, *Nat. Rev. Cancer* 2004, **4**, 592-603.